applied sciences

MDPI

Article

Evaluation Method for Determining Rock Brittleness in Consideration of Plastic Deformation in Pre-Peak and Failure Energy in Post-Peak

Xiaopeng Yue [1,2,3], Tao Wen [1,2,*], Yuan Gao [4], Wenjun Jia [1], Yankun Wang [1,2] and Mingyi Hu [1,2]

[1] School of Geosciences, Yangtze University, Wuhan 430100, China; hr@zpetro.cn (X.Y.); 2022710489@yangtzeu.edu.cn (W.J.); ykwang@yangtzeu.edu.cn (Y.W.); humingyi65@163.com (M.H.)
[2] Jiacha County Branch, Hubei Yangtze University Technology Development Co., Ltd., Shannan, Tibet 856499, China
[3] Zhongguan Chenhua Petroleum Engineering Co., Ltd., Wuhan 430073, China
[4] Faculty of Engineering, China University of Geosciences, Wuhan 430074, China; gy201606nb@163.com
* Correspondence: wentao200840@yangtzeu.edu.cn

Abstract: The assessment of rock brittleness holds significant importance for understanding and predicting the mechanical properties and engineering behavior of rocks. Due to the lack of a unified definition of rock brittleness, numerous evaluation methods for brittleness indexes have been proposed by scholars both domestically and internationally in recent decades, resulting in diverse evaluation outcomes. In this study, we first summarize the existing rock brittleness evaluation methods and highlight their respective advantages and disadvantages. Subsequently, considering the pre-peak plastic deformation of the rock mass, the pre-peak brittleness index factor is introduced. Furthermore, taking into account the total energy consumed by the rock mass for failure after the peak, the post-peak brittleness index factor is proposed. These two components of the brittleness index describe the characteristics of different stages of the stress-strain curve, leading to the development of a novel brittleness index. The proposed method is then applied to evaluate the brittleness of both red-bed sandstone and cyan sandstone, revealing the variation of rock brittleness under different working conditions. Finally, three existing evaluation methods are selected to validate the rationality of the proposed method. The results demonstrate that for red-bed sandstone, the proposed brittleness index exhibits maximum values under natural conditions at all confining pressures. The four brittleness indexes consistently characterize the brittleness of red-bed sandstone under natural conditions. Under saturated conditions, the brittleness indexes exhibit different patterns of variation. For cyan sandstone, the three brittleness indexes—B7, B9, and Bnew—exhibit a similar trend in characterizing the brittleness of cyan sandstone under natural conditions and freezing-thawing conditions, while the trend of B17 is essentially opposite to that of the previous three indexes. The research findings provide guidance for the assessment of sandstone brittleness.

Keywords: rock brittleness; plastic deformation; sandstone; energy dissipation; brittleness index

Citation: Yue, X.; Wen, T.; Gao, Y.; Jia, W.; Wang, Y.; Hu, M. Evaluation Method for Determining Rock Brittleness in Consideration of Plastic Deformation in Pre-Peak and Failure Energy in Post-Peak. *Appl. Sci.* **2023**, *13*, 12711. https://doi.org/10.3390/app132312711

Academic Editor: Nikolaos K. Koukouzas

Received: 25 October 2023
Revised: 24 November 2023
Accepted: 24 November 2023
Published: 27 November 2023

1. Introduction

The evaluation of rock brittleness holds significant research significance in the field of academic studies [1,2]. Understanding the brittleness characteristics of rocks is crucial for various applications, such as geotechnical engineering, rock mechanics, and petroleum reservoir characterization [3,4]. Evaluating rock brittleness helps in predicting rock failure behavior, designing safe and stable structures, optimizing drilling and hydraulic fracturing operations, and assessing the potential for induced seismicity [5–7].

Currently, numerous studies have been conducted to investigate rock brittleness evaluation methods [2]. These studies have proposed various approaches, including

empirical indexes, laboratory testing, and numerical modeling techniques [2,3,8]. Empirical indexes often rely on simple parameters, such as the ratio of compressive to tensile strength or the strength ratio index, to estimate rock brittleness [9,10]. Laboratory testing involves conducting experiments, such as uniaxial or triaxial compression tests, to analyze the stress-strain behavior and failure patterns of rocks [11–13]. Numerical modeling techniques utilize advanced computational methods, such as finite element analysis or discrete element modeling, to simulate rock behavior and predict brittleness. Brittleness indexes based on mineral composition vary with the classification criteria of brittle minerals and do not consider the influence of rock diagenesis and strength components on rock brittleness [1,3,14]. Although brittleness indexes based on mechanical properties take into account the influence of rock mass strength characteristics, they are not suitable for evaluating the brittleness characteristics of different types of rocks and complex stress conditions in the rock mass [5,6]. Brittleness indexes based on the characteristics of the complete stress-strain curve can reflect the influence of crack propagation on rock failure deformation during the rock's damage process but fail to explain the strength evolution process of the rock [7,12]. Brittleness indexes based on hardness testing are primarily used for the brittleness evaluation of homogeneous materials, and the heterogeneity and anisotropy of rocks inevitably result in significant deviations in brittleness evaluation in such cases [7]. Despite the progress made in rock brittleness evaluation, challenges still exist. The complex nature of rock behavior, including heterogeneity, anisotropy, and nonlinear stress-strain relationships, poses difficulties in accurately assessing brittleness [15,16]. Additionally, the lack of standardized brittleness evaluation criteria and the need for integrating multiple parameters for comprehensive assessments remain areas of active research.

In light of these research gaps, this study aims to contribute to the field of rock brittleness evaluation by proposing a novel method that incorporates energy considerations into the assessment. By analyzing the stress-strain curve characteristics before and after the peak stress, this method provides a more physically meaningful approach to quantifying rock brittleness. The findings of this study will enhance our understanding of rock failure mechanisms and provide valuable insights for engineering and geoscience applications.

2. The Existing Methods for Determining Rock Brittleness

Brittleness evaluation plays a significant role in assessing the mechanical behavior of rocks for various engineering applications [2]. This section aims to discuss the current state of the research of rock brittleness assessment and critically analyze the advantages and disadvantages of different approaches based on mineral composition, strain, stress, elastic parameter, and energy. Table 1 shows the existing methods for determining the rock brittleness.

(a) Definition of Brittleness Index based on Stress

The stress-based approach defines rock brittleness in terms of stress levels at failure or the stress intensity required for crack propagation. This method allows for the assessment of the rock's resistance to fracturing under different loading conditions. The advantage of stress-based definitions is their direct relationship with fracture initiation and propagation. However, accurately determining stress levels in rocks can be challenging, particularly in heterogeneous formations.

Table 1. The existing methods for determining the rock brittleness.

Methods	Symbol	Types
$B_1 = \sigma_c/\sigma_t$ $B_2 = (\sigma_c - \sigma_t)/(\sigma_c + \sigma_c)$ $B_3 = \sqrt{\sigma_c\sigma_t/2}$ $B_4 = \sigma_c\sigma_t/2$ $B_5 = \sin\alpha$ $B_6 = 45^\circ + \alpha/2$ $B_7 = (\sigma_p - \sigma_r)/\sigma_p$ $B_8 = (\varepsilon_r - \varepsilon_p)/\varepsilon_p$ $B_9 = \frac{(\sigma_p-\sigma_r)/\sigma_p}{(\varepsilon_r-\varepsilon_p)/\varepsilon_p}$ $B_{10} = \frac{(\sigma_p-\sigma_r)(\varepsilon_r-\varepsilon_p)}{\varepsilon_p\sigma_p} + \frac{\sigma_p-\sigma_r}{\varepsilon_r-\varepsilon_p}$	σ_t is tensile strength, σ_c is UCS, α is internal friction angle, σ_p, σ_r are peak strength (PS) and residual strength, $\varepsilon_r, \varepsilon_p$ are peak strain and residual strain	Based on stress and strain (B_1–B_{10}) [2,10]
$B_{11} = E_I + \mu_I$ $B_{12} = \frac{E_I}{\mu_I}$ $B_{13} = \frac{M_I - E_I}{M_I}$ $B_{14} = \frac{E_I}{M_I}$	E_I, μ_I are elastic modulus and Poisson's ratio, M_1 is the post-peak secant modulus	Based on elastic parameters (B_{11}–B_{14}) [2]
$B_{15} = \frac{W_r}{W}$ $B_{16} = \frac{\sigma_p-\sigma_r}{\varepsilon_r-\varepsilon_p} + \frac{W_r}{W}$ $B_{17} = \frac{W_{post}^{out}}{W}$ $B_{18} = \frac{W_r}{W_{post}^{out}}$ $B_{19} = \frac{W_d}{W_{post}^{out}}$ $B_{20} = \frac{2W_r}{(\sigma_p-\sigma_r)(\varepsilon_r-\varepsilon_p)} \times \frac{\varepsilon_{ci}}{\Delta\varepsilon}$	W_r, W are elastic strain energy and total absorption energy before peak strength, W_{post}^{out} is elastic strain energy used for post − peak crack expansion, W_d is dissipation energy before peak strength, ε_{ci} is initial strain, ε_{ci} is plastic strain	Based on energy (B_{15}–B_{20}) [5,6]
$B_{21} = \frac{C_{brit}W_{pre}^{ce}}{C_{brit}W_{pre}^{ce} + C_{inbrit}W_{pre}^{out}}$ $B_{22} = \frac{C_{brit}\left(W_{pre}^{ce} - W_{post}^{re}\right)}{C_{brit}\left(W_{pre}^{ce} - W_{post}^{re}\right) + C_{inbrit}W_{post}^{in}}$ $B_{23} = \frac{\alpha_i C_{brit}}{C_{total}}$ $B_{24} = \frac{(W_{qtz}+W_{carb})}{W_{total}}$	C_{brit} is the content of brittle minerals, C_{inbrit} is the content of non − brittle minerals, W_{post}^{re} is residual elastic strain energy, W_{post}^{ce} is elastic strain energy and total absorption energy before peak strength, W_{pre}^{out} is dissipation energy consumed for crack closure and friction C_{total} is the content of all minerals, α_i is the correction value corresponding to different minerals, W_{qtz} is the quartz content, W_{carb} is the feldspar content, W_{total} is the total mineral content	Based on mineral composition (B_{21}–B_{24}) [2,5,6]

(b) Definition of Brittleness Index based on Strain

Another approach to evaluating rock brittleness is through strain-based definitions. This method focuses on quantifying the deformation characteristics of rocks under stress. By considering the strain at failure or the strain energy release, this approach provides insights into the rock's ability to undergo plastic deformation before failure. The advantage of strain-based definitions is their ability to capture the ductility or plasticity of rocks [17,18]. However, their drawback lies in the complexity of strain measurements and the need for advanced testing equipment.

(c) Definition of Brittleness Index Based on Elastic Parameters

Another approach involves defining brittleness indexes using elastic deformation parameters, such as Young's modulus and Poisson's ratio. These parameters reflect the rock's ability to undergo elastic deformation without fracturing. This approach provides a more direct connection to rock mechanics properties and can be determined through laboratory testing or empirical correlations. However, it neglects the influence of plastic deformation and post-peak behavior, limiting its ability to capture the complete brittleness spectrum.

(d) Definition of Brittleness Index based on Energy

The energy-based definition of rock brittleness focuses on quantifying the fracture energy or the energy required to propagate cracks within rocks [19–22]. This approach considers the relationship between the energy dissipated during fracture and the rock's brittleness characteristics. The advantage of energy-based definitions is their ability to capture the rock's fracture toughness and resistance to crack propagation. However, accurately measuring fracture energy necessitates sophisticated experimental setups and can be time-consuming.

(e) Definition of Brittleness Index based on Rock Mineral Composition

One approach to defining rock brittleness is by considering the mineral composition. This method involves characterizing the rock's brittleness index based on the proportions and mechanical properties of its constituent minerals. The advantage of this approach is its ability to capture the influence of mineralogy on rock behavior. However, its major limitation lies in the difficulty of accurately quantifying the mineral composition and establishing consistent correlations between mineralogy and brittleness.

Based on Figure 1, the shortcomings of the current brittleness evaluation method based on stress-strain curves can be identified. For lines 1 and 2, they exhibit the same stress drop after the peak but have different slopes before the peak. If only the post-peak portion of the stress-strain curve is considered, it would inevitably lead to the calculation of the same brittleness index. Clearly, this type of brittleness index is not suitable. For lines 1 and 3, they have the same slope before the peak but different peak strengths and different stress drops after the peak. If the brittleness index is calculated based on the pre-peak elastic modulus, it neglects the influence of the post-peak curve on rock brittleness. It is evident that this type of brittleness index is not appropriate. For lines 2 and 4, they have the same slope before the peak, the same stress drop after the peak, but different peak strengths. If only the post-peak portion of the stress-strain curve and the pre-peak elastic deformation are considered, it overlooks the influence of the rock's inherent peak strength. Clearly, this type of brittleness index is not suitable. For lines 3 and 4, they have different slopes before the peak, different stress drops after the peak, but the same peak strength and the same post-peak slope. Most brittleness indexes also fail to reflect this characteristic. Therefore, it is necessary to propose a brittleness index that can simultaneously reflect the pre-peak and post-peak curve characteristics and capture the elastic and plastic deformation features during the rock failure process.

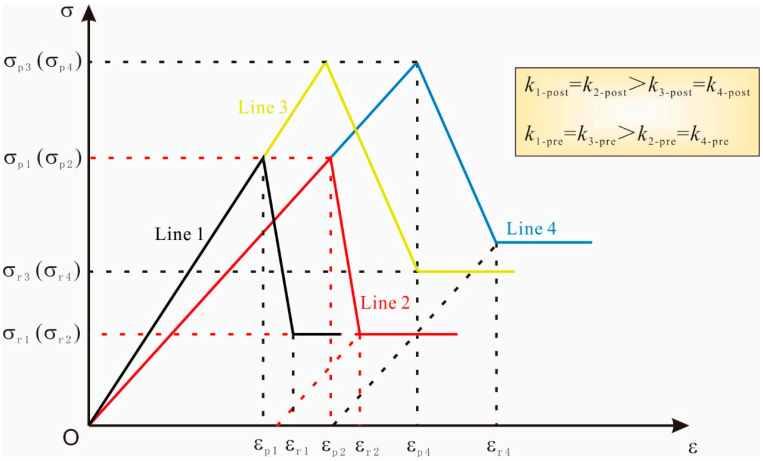

Figure 1. Simplified stress-strain curves.

3. A Method to Evaluate the Brittleness in Consideration of Plastic Deformation in Pre-Peak and Failure Energy in Post-Peak

In the evaluation of rock brittleness, it is essential to consider both pre-peak and post-peak stress-strain curves. This is because the behavior of rocks during the pre-peak and post-peak stages provides valuable insights into their brittleness characteristics.

During the pre-peak stage, the rock undergoes elastic deformation and initial crack propagation. By analyzing the stress-strain curve in this stage, we can determine the elastic modulus, which represents the rock's stiffness and ability to withstand deformation without fracturing. The elastic modulus is a crucial parameter in defining the rock's brittleness, as a higher modulus indicates a more brittle behavior. The inclusion of pre-peak plastic deformation in the brittle evaluation method is necessitated by the recognition that rocks often exhibit significant ductility before reaching their peak strength. By quantifying the extent of plastic deformation prior to failure, this method captures the rock's ability to deform without fracturing. This information is essential for engineering design, as it helps identify potential failure modes and select appropriate mitigation measures.

After reaching the peak stress, the rock experiences post-peak behavior characterized by progressive failure and plastic deformation. By examining the stress-strain curve in this stage, we can assess the extent of plastic deformation, energy absorption, and the ability to undergo ductile deformation. These parameters influence the rock's brittleness, as a higher degree of plastic deformation and energy absorption indicates a more ductile behavior. The consideration of post-peak failure energy in the brittle evaluation method is crucial as it provides insights into the rock's fracture toughness and energy dissipation capacity. By quantifying the energy required for crack propagation and failure, this approach can assess the rock's resistance to catastrophic failure and its ability to absorb and dissipate energy. Such information is vital for optimizing engineering designs and ensuring the stability of rock structures.

Considering both pre-peak and post-peak stress-strain curves allows for a comprehensive evaluation of rock brittleness. It provides a holistic understanding of the rock's mechanical response to stress, including its initial stiffness, crack propagation, and ability to undergo plastic deformation. By analyzing the entire stress-strain curve, we can capture the complete spectrum of brittleness and understand the rock's failure mechanisms.

Based on the definitions provided by existing scholars, this study considers brittleness and ductility as opposing characteristics [17,18]. The strain occurring in the rock mass prior to failure can be divided into recoverable elastic strain and irrecoverable plastic strain induced by crack propagation. The higher the degree of plastic deformation, the lower the brittleness of the rock mass, while the brittleness is independent of the amount of elastic deformation during the failure process. Therefore, if the amount of plastic strain occurring prior to failure is minimal, the rock mass is considered more brittle. As shown in Figure 2,

the brown area represents the stored elastic strain energy prior to failure, and the slope of the line dividing the yellow area and the brown area corresponds to the elastic modulus. Hence, $2W_e/E$ can be used to obtain the elastic strain occurring prior to failure, while the deformation prior to failure consists of plastic deformation and elastic deformation. Therefore, subtracting the elastic deformation from the total strain prior to failure provides the plastic deformation prior to failure, thus evaluating the brittleness value of the rock mass. The formula for the pre-peak brittleness index is given as follows:

$$B_{pre} = log\left(\frac{1}{\varepsilon_p - \frac{2W_e}{E}}\right), \tag{1}$$

where ε_p is the strain before peak strength, W_e is the elastic strain energy, and E is the elastic modulus. Herein, the log symbol represents the log for the decadic logarithm.

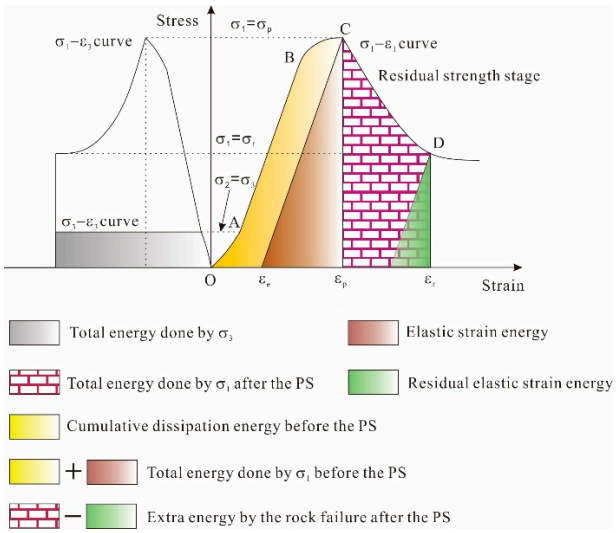

Figure 2. Schematic diagram of energy evolution for different stages.

Analyzing the brittleness of rock masses solely from an energy perspective prior to the peak does not allow for distinguishing between the energy required to overcome cohesive forces and the energy needed for friction and heat generation. Therefore, in this study, the brittleness of the rock mass after the peak is assessed based on plastic strain. This approach provides a comprehensive evaluation considering the specific energy consumed during crack propagation and accounts for the rock mass's post-peak behavior.

The post-peak brittleness index represents the total strain energy required for failure after reaching the peak stress. The difference in crack propagation between brittle and non-brittle rocks during the failure process using a schematic diagram is demonstrated. It can be observed that brittle materials require less energy for crack propagation, while non-brittle materials require energy to sustain crack growth. Therefore, the lower the energy required for crack propagation in the post-peak stage, the higher the brittleness of the rock mass. As shown in Figure 2, the energy absorbed by the rock mass prior to the peak is divided into dissipation energy (yellow area) used for crack propagation, overcoming cohesive forces, friction, and heat dissipation, and the stored elastic strain energy (brown area) of the rock mass. Some of the stored elastic energy is utilized for crack propagation after the peak, while the remaining portion is residual elastic energy (green area). The energy for rock mass failure after the peak includes not only the stored elastic energy prior to the peak but also the external energy input after the peak (wall shape). Therefore, the total energy for post-peak rock mass failure is given by (brown area + green area − green area), which can be expressed as $W_e + W_{out} - W_{re}$. However, $W_e + W_{out} - W_{re}$ is inversely

proportional to the brittleness of the rock mass. Therefore, the reciprocal form is used to express the brittleness of the rock mass.

$$B_{post} = log\frac{1}{W_e + W_{out} - W_{re}}, \quad (2)$$

where W_e is the stored elastic strain energy before the peak, W_{out} is the external energy input after the peak, and W_{re} is the residual elastic strain energy.

In this study, a logarithmic function is employed to reduce the numerical disparity between the two components of the brittleness index, thus avoiding the influence of one component's magnitude on the magnitude of the other component. For the coupling of the two brittleness index components, a multiplication form is selected, following the same principle as mentioned earlier. Additionally, the two components of the brittleness index describe the characteristics of stress-strain curve at different stages. Therefore, based on the energy parameters at the pre-peak and post-peak stages, the proposed brittleness index in this study is presented as follows:

$$B_{new} = B_{pre} \times B_{post} \quad (3)$$

4. Verification of the Brittleness Indexes

4.1. For Red-Bed Sandstone under Saturated Condition

This study validates the brittleness evaluation using red-bed sandstone. The red-bed sandstone underwent triaxial compression tests under different confining pressures in its natural state and in its saturated state. The experimental process for red-bed sandstone under saturated conditions was as follows: the samples were divided into two groups, totaling eight samples. The first group underwent saturation testing, while no further operations were required for the second group. In the saturation test, the samples were placed in a water tank for natural absorption. Initially, water was injected to a height of 1/4 of the specimen and, every 2 h, water was injected to heights of 1/2 and 3/4 of the specimen. After 6 h, the samples were fully submerged, and after 48 h of water absorption, they were dried in a drying oven before testing. Each group of samples underwent triaxial compression tests under confining pressures of 2, 4, 8, and 16 MPa, resulting in stress-strain curves, as shown in Figure 3.

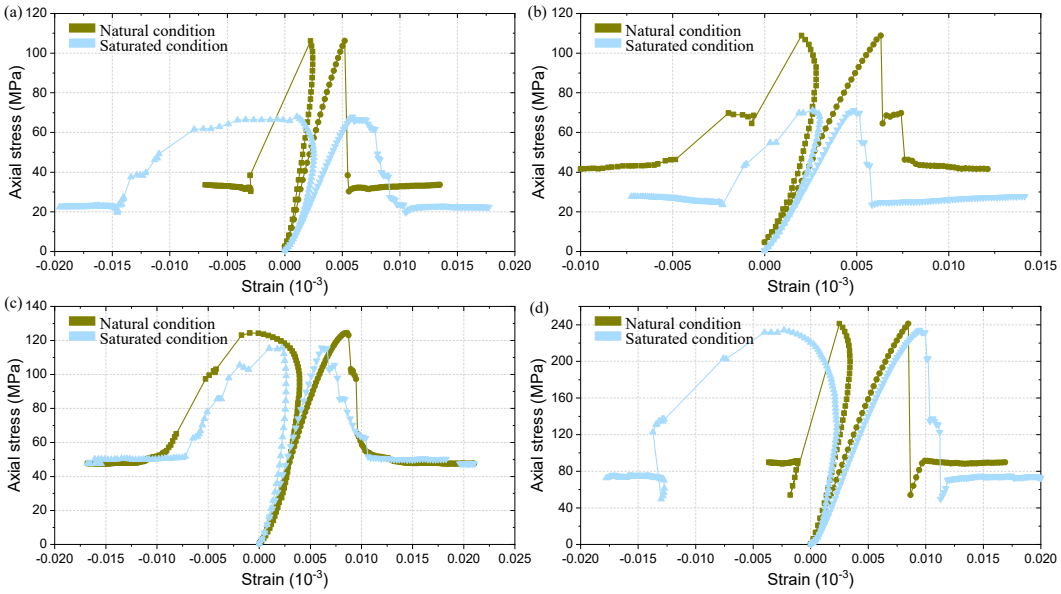

Figure 3. The stress-strain curves of red-bed sandstones under different confining pressures: (**a**) 2 MPa; (**b**) 4 MPa; (**c**) 8 MPa; (**d**) 16 MPa.

From the graph, it is evident that under confining pressures of 2, 4, 8, and 16 MPa, the post-peak curve is roughly similar, especially showing a multi-step downward trend under saturated conditions, while the peak strength of red-bed sandstone in its natural state is significantly higher than that of red-bed sandstone under saturated condition. After saturation, the strength of the sandstone deteriorates, and under low confining pressure, the degree of deterioration is higher. Furthermore, based on the axial strain-axial stress curve, it can be observed that the total strain of red-bed sandstone in its natural state is significantly lower than that of red-bed sandstone under saturated condition. This indicates that the brittleness is higher in its natural state compared to that under saturated conditions.

Using the brittleness index formula proposed in this study, the brittleness values of red-bed sandstone under different confining pressures in its natural state and in its saturated condition can be calculated based on the stress-strain curves mentioned above. The results are shown in Figure 4. It can be observed that under natural conditions, the brittleness values of red-bed sandstone increased by 18.52% from 2 MPa to 4 MPa, 62.59% from 4 MPa to 8 MPa, and 48.65% from 8 MPa to 16 MPa. Under saturated conditions, the brittleness value increased by 50.22% from 2 MPa to 4 MPa, decreased by 78.93% from 4 MPa to 8 MPa, and decreased by 52.50% from 8 MPa to 16 MPa. Under saturated conditions, compared to the natural state, the brittleness values decreased by 21.55%, 75.17%, and 88.21% for 2 MPa, 8 MPa, and 16 MPa, respectively. Under saturated conditions at 4 MPa confining pressure, the brittleness value increased by 17.85% compared to the natural state. Therefore, both in the natural state and under saturated conditions, the brittleness index of red-bed sandstone decreases with increasing confining pressure, which is consistent with the trend of decreasing brittleness with increasing confining pressure in rock masses. However, an anomalous phenomenon is observed in the brittleness under saturated conditions at 4 MPa, which is believed to be attributed to experimental errors caused by sample collection. Overall, the brittleness of red-bed sandstone under saturated conditions is lower compared to its natural state.

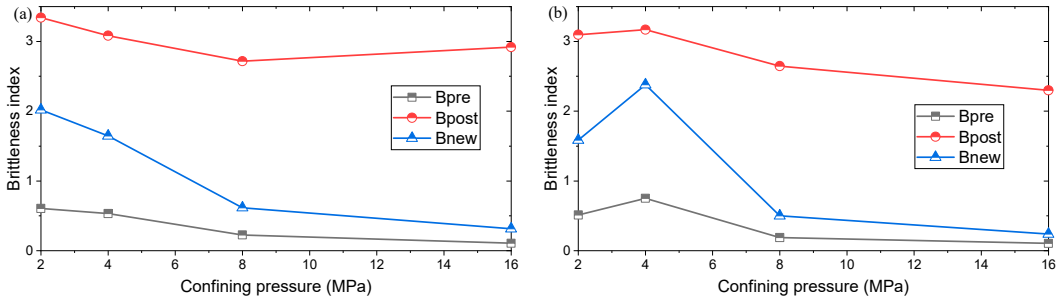

Figure 4. The brittleness index of red-bed sandstones: (**a**) Under natural conditions; (**b**) Under saturated conditions.

4.2. For Cyan Sandstone under Freezing-Thawing Condition

To validate the feasibility of the proposed method, another type of rock—cyan sandstone—collected from different regions, was used in this study. Triaxial compression tests were conducted under natural conditions and freezing-thawing conditions, with confining pressures set at 0, 3, 6, 9, and 12 MPa. The stress-strain curves of cyan sandstone under natural conditions and freezing-thawing conditions at these confining pressures are shown in Figure 5. From the graph, it can be observed that, under natural conditions, both the peak strength and the residual strength of cyan sandstone gradually increase with increasing confining pressure. This trend is also observed under freezing-thawing conditions. At the same confining pressure, the peak strength of the rock after freezing-thawing is significantly lower than that under natural conditions, while the difference in residual strength is not significant. For 0 and 3 MPa, the peak strain of the rock after freezing-thawing is significantly higher than that under natural conditions, while for high confining pressure, the peak strain difference between the two is smaller than that

under low confining pressure. This may be because the confining pressure suppresses the deformation of the rock. Clearly, during the initial compaction stage, the stress-strain curve shows a distinct upward concavity. In this stage, the initial cracks inside the rock gradually close under pressure until compaction is no longer possible, accumulating energy gradually. In the post-peak stage, the rock exhibits significant brittleness, with a noticeable stress drop, indicating that characterizing rock brittleness through stress-strain curves before and after the peak stress is feasible.

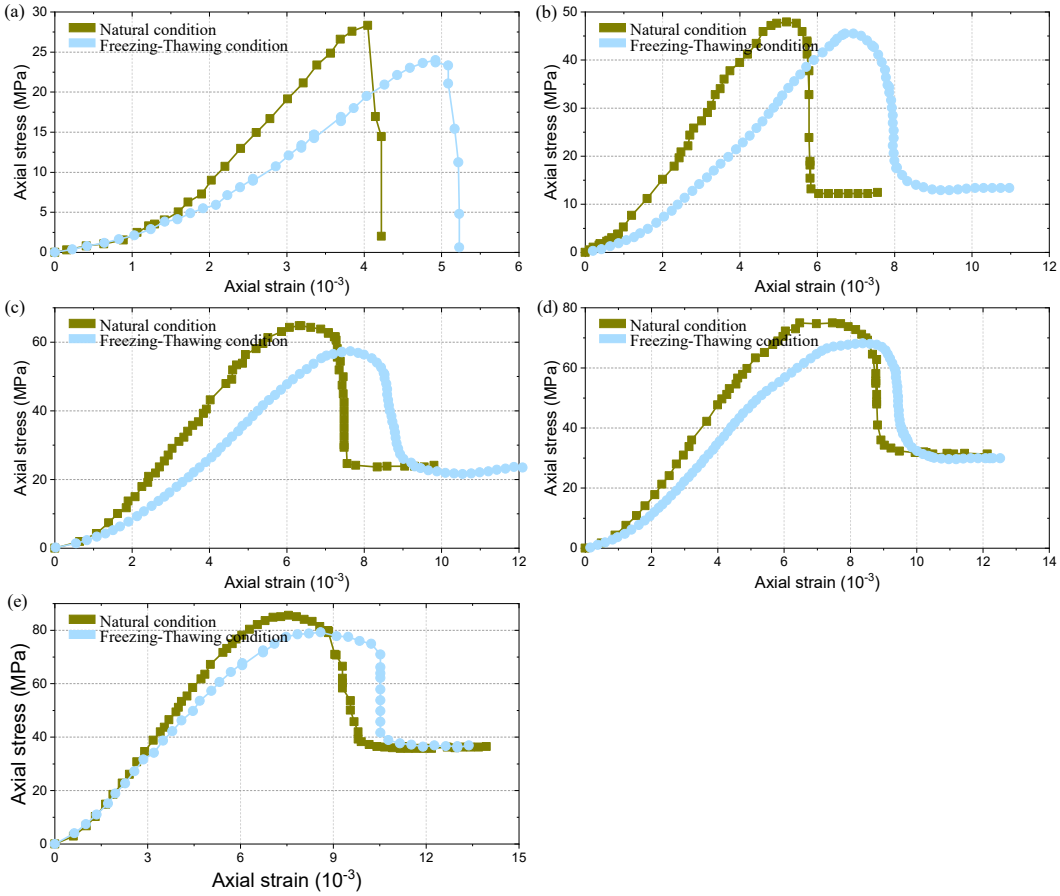

Figure 5. The stress-strain curves of cyan sandstones under different confining pressures: (**a**) 0 MPa; (**b**) 3 MPa; (**c**) 6 MPa; (**d**) 9 MPa; (**e**) 12 MPa.

The brittleness indexes calculated using the proposed formulas are shown in Figure 6. Under natural conditions, the pre-peak brittleness index, post-peak brittleness index, and overall brittleness index generally increase with increasing confining pressure, except for the pre-peak brittleness index at 3 MPa confining pressure, which is higher than the pre-peak brittleness index at 0 MPa confining pressure. This is because under a confining pressure of 3 MPa, the pre-peak curve has a weak corrective effect on the rock brittleness. Overall, the pre-peak brittleness index is significantly higher than the post-peak brittleness index. Furthermore, the trend of Bnew is basically consistent with Bpost, and its value is not significantly different, indicating that the post-peak brittleness index contributes more to the rock's brittleness, while the pre-peak brittleness index plays a supporting role in adjusting the size of Bnew. Similar trends are observed under freezing-thawing conditions. Additionally, at the same confining pressure, the brittleness indexes under natural conditions are higher than those under freezing-thawing conditions. Specifically, under freezing-thawing conditions at 0 MPa, 3 MPa, 6 MPa, 9 MPa, and 12 MPa, the brittleness indexes of cyan sandstone decrease by 8.69%, 31.39%, 17.00%, 13.57%, and 15.69%, respectively, compared to the brittleness indexes under natural conditions. In

conclusion, the brittleness of cyan sandstone decreases with increasing confining pressure, and freezing-thawing action can reduce the brittleness of the rock.

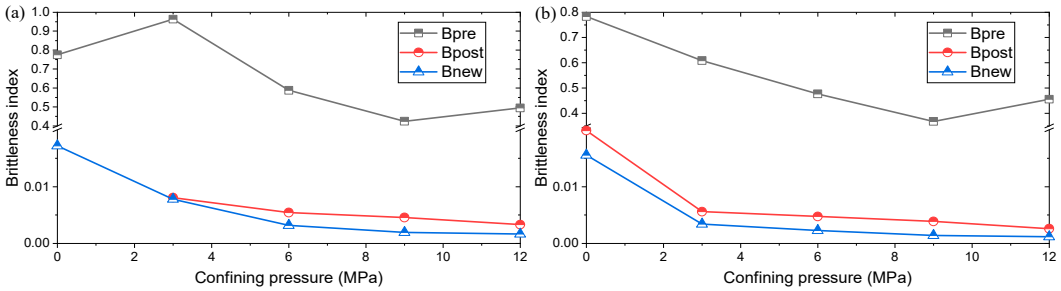

Figure 6. The brittleness index of cyan sandstones: (**a**) Under natural condition; (**b**) Under freezing-thawing conditions.

5. Comparison of Brittleness Index with Other Existing Methods

As shown in Figure 7, the changes in brittleness under different confining pressures for red-bed sandstone under saturated conditions and in its natural state were evaluated using B7, B9, and B17, which were compared to the brittleness evaluation method proposed in this study. Brittleness indexes B7 and B9 based on stress-strain parameters are selected to evaluate rock brittleness, while B17 is a brittleness index proposed based on energy parameters. The above three indexes have been validated by numerous cases, demonstrating their ability to evaluate rock brittleness [2,10]. Therefore, the rationality of the proposed method is verified through various different definitions of brittleness indexes. Due to the different orders of magnitude of the various brittleness indexes, the brittleness indexes of each method were standardized to facilitate the presentation of their respective trends. In Figure 7, under natural conditions, the proposed brittleness index in this study exhibits the maximum values at all confining pressures, with the lowest value observed for B7. Furthermore, the magnitude of decrease in values for B7 and B9 diminishes as the confining pressure increases. The four brittleness indexes consistently characterize the brittleness of the red-bed sandstone under natural conditions. Under saturated conditions, the brittleness indexes exhibit different patterns of variation. The values of the proposed brittleness index, in comparison with the other indexes, fall within the intermediate range, and their trends of change are generally consistent.

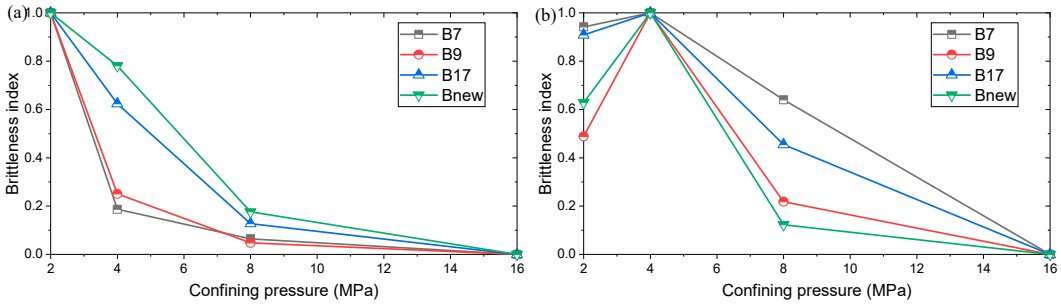

Figure 7. Comparison of the brittleness indexes for red-bed sandstones after normalization: (**a**) Under natural conditions; (**b**) Under saturated conditions.

Compared to B7 and B9, the advantages of the brittleness evaluation proposed in this study are as follows: the proposed method describes the stress-strain curve characteristics before and after the peak stress, and compared to B7 and B9, which use the stress increment after the peak stress and the slope of the curve to describe the brittleness of rock masses, the use of rock mass energy in this study for evaluating brittleness is more physically meaningful. This study argues that the stress growth rate and stress-strain rate only indicate the strength characteristics of the rock mass, without a direct relationship with

brittleness. However, analyzing the characteristics of rock mass failure from an energy perspective can better reflect the brittleness characteristics of the rock mass. Compared to the brittleness evaluation proposed in this study, B17 lacks the characteristics after the peak stress and uses the proportion of elastic energy to evaluate the brittleness of the rock mass, which would give an advantage to highly elastic rock masses. Therefore, the study suggests that if energy is used to evaluate the brittleness of rock masses, it should be based on the amount of energy consumed by the rock mass in overcoming friction and heat release.

As shown in Figure 8, the changes in brittleness under different confining pressures for cyan sandstone under freezing-thawing conditions and in its natural state were evaluated using B7, B9, and B17, which were compared to the brittleness evaluation method proposed in this study. Due to the different orders of magnitude of the various brittleness indexes, the brittleness indexes of each method were standardized to facilitate the presentation of their respective trends. Under natural conditions, the three brittleness indexes, B7, B9, and Bnew, exhibit a similar trend in characterizing the brittleness of the cyan sandstone. They gradually decrease with increasing confining pressure, and the value of Bnew is larger than B9 and B7. However, the trend of B17 is essentially larger than the previous three indexes, as it decreases gradually with increasing confining pressure at a relatively uniform rate. Under freezing-thawing conditions, the variation patterns of the three brittleness indexes, B7, B9, and Bnew, are similar, and the value of Bnew also falls between B9 and B7. At lower confining pressures, the three brittleness indexes show a greater rate of decrease, and as the confining pressure increases, their rate of decrease tends to stabilize. Similarly, the trend of B17 is essentially opposite to the previous three indexes.

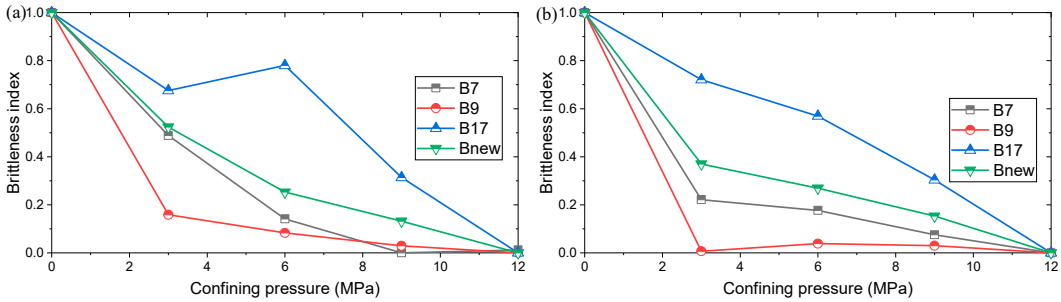

Figure 8. Comparison of the brittleness indexes for cyan sandstones after normalization: (**a**) Under natural conditions; (**b**) Under freezing-thawing conditions.

In Figure 9, the *x*-axis represents the normalized brittleness indexes, where 1 represents the normalized brittleness index B7′, 2 represents B9′, 3 represents B17′, and 4 represents Bnew′. Comparing the normalized brittleness indexes reflects the variations in rock brittleness under different conditions. From the graph, it can be observed that, for the red-bed sandstone, under natural conditions, the brittleness gradually weakens with increasing confining pressure, indicating that confining pressure has an inhibitory effect on the brittleness of red-bed sandstone. However, under the influence of water–rock interaction, the brittleness initially increases and then decreases with increasing confining pressure, suggesting that the brittleness of red-bed sandstone changes after water–rock interaction. This change is more pronounced under isotropic conditions, and the brittleness enhances under anisotropic conditions.

As for the cyan sandstone, it is evident that the change trend of the brittleness index Bnew′ is consitent with the other three indexes. For example, at a confining pressure of 3 MPa, after freezing-thawing action, the radii of the spheres representing B7′, B9′, and Bnew′ are significantly smaller than those under natural conditions, indicating that freezing-thawing action accelerates the rate of brittle-ductile transition in the cyan sandstone.

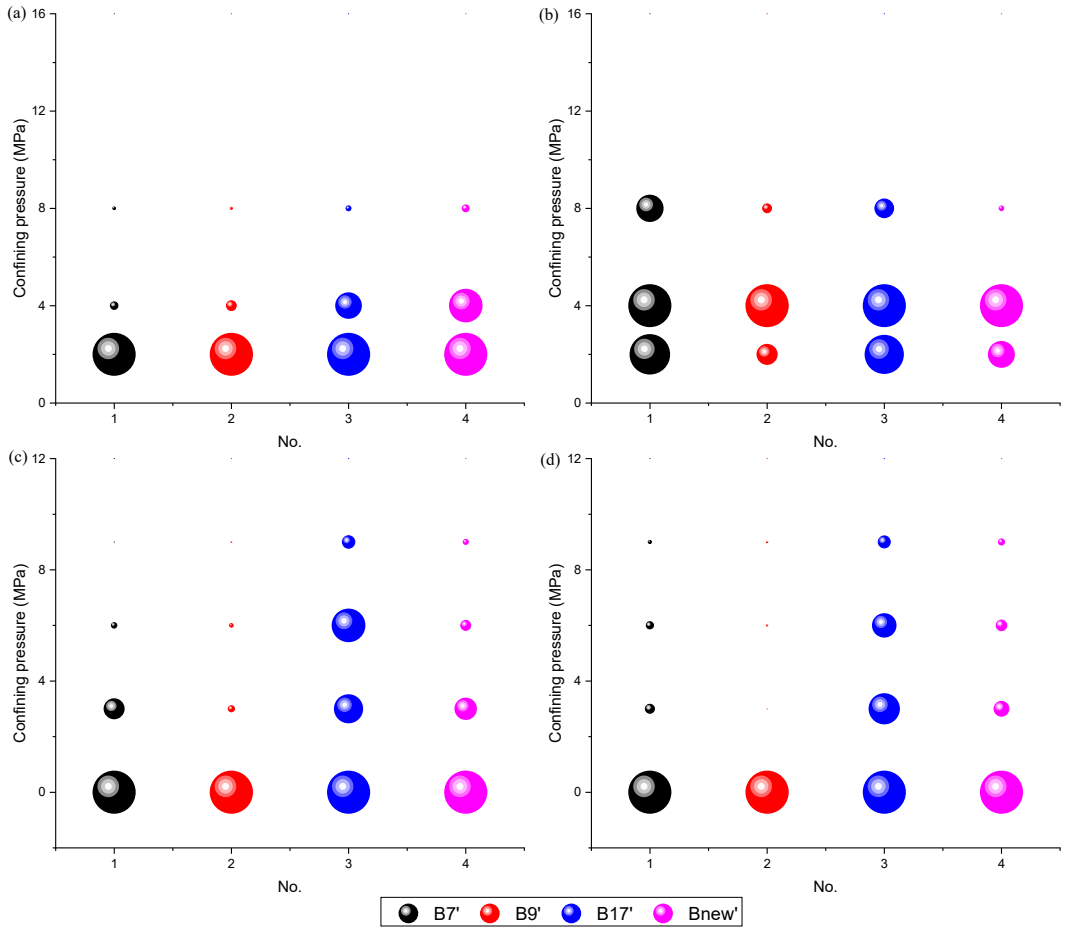

Figure 9. Comparison of the brittleness indexes for different rock types: (**a**) Red-bed sandstone under natural condition; (**b**) Red-bed sandstone under saturated condition; (**c**) Cyan sandstone under natural condition; (**d**) Cyan sandstone under freezing-thawing condition.

6. Discussion

6.1. Rock Failure Mechanism from the Energy Evolution

The transformation of rock brittleness and ductility depends on factors such as stress level, physical properties of the rock (including crack density and rock toughness), mechanical properties of the rock (including tensile strength and shear strength), and loading rate. These factors collectively determine the rock's failure behavior and mechanical response under stress. According to the proposed brittleness index in this study, during the evolution from absolute ductility to absolute brittleness, both pre-peak dissipated energy and post-peak fracture energy gradually decrease. As shown in Figure 10, two characteristic points exist in this process: the ductility characteristic point ($E > -M = Q$) and the moderate brittleness characteristic point ($E = -M > Q$). Based on these two characteristic points, the brittleness characteristics of the rock during the entire failure process can be classified as follows: absolute ductility ($E > Q = M = 0$), weak brittleness ($E > -M > Q$), strong brittleness ($-M > E > Q$), and extremely strong brittleness ($E > M > Q$).

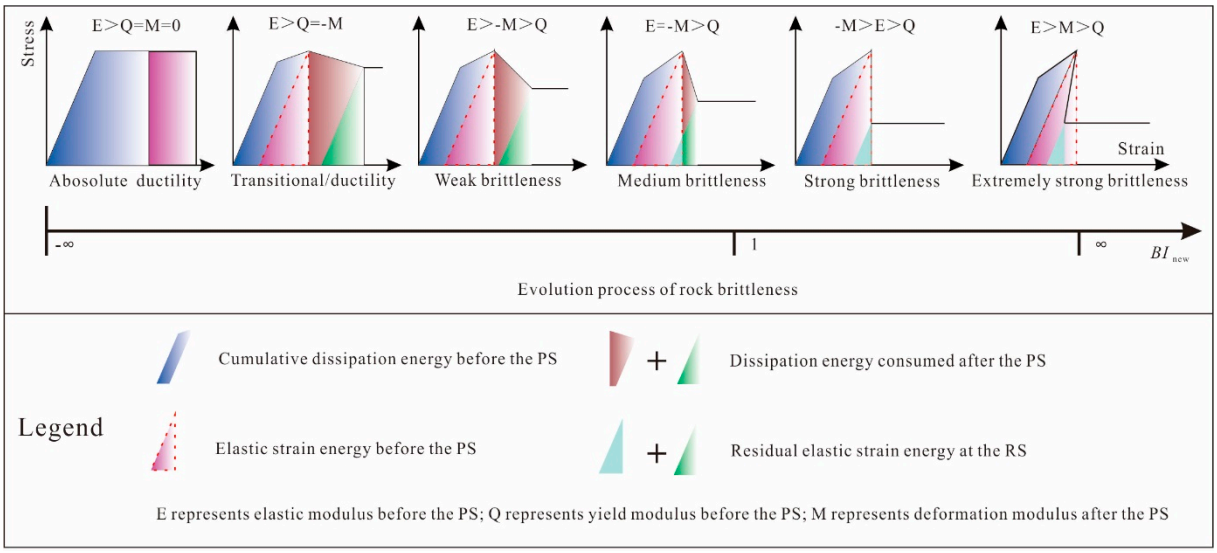

Figure 10. Evolution process of the brittleness index BI_{new}.

The understanding of rock failure mechanisms is fundamental to evaluating rock brittleness and implementing appropriate engineering interventions [23,24]. This section focuses on elucidating the mechanisms of rock failure from the perspective of energy evolution. By examining energy redistribution, dissipation, and release during the progressive failure process, a comprehensive understanding of rock brittleness can be achieved. The discussion emphasizes the significance of energy-based analysis and its implications for engineering applications.

(a) Energy Redistribution during Rock Failure

Rock failure is often accompanied by energy redistribution within the rock mass [25]. This redistribution occurs due to stress concentration and the initiation and propagation of cracks. Energy-based analysis allows for quantifying the redistribution of potential and kinetic energy, providing insights into the spatial and temporal evolution of failure. By understanding energy redistribution, engineers can anticipate potential failure zones, optimize support systems, and design effective reinforcement measures.

(b) Energy Dissipation during Rock Failure

Energy dissipation plays a crucial role in rock failure processes. As cracks propagate and interact, energy is dissipated through various mechanisms, such as friction, microcracking, and fracture surface roughness. Energy-based analysis enables the quantification of dissipated energy, helping to assess the brittleness of rocks. The measurement of energy dissipation provides valuable information for designing energy-absorbing structures and selecting suitable materials to enhance rock stability.

(c) Energy Release during Catastrophic Rock Failure

Catastrophic failure events, such as rockbursts and collapses, involve the sudden release of stored energy. Energy-based analysis allows for understanding the magnitude and spatial distribution of released energy during such events. This information is crucial for assessing the potential impact on surrounding structures and developing effective hazard mitigation strategies. By quantifying energy release, engineers can optimize support systems, implement real-time monitoring, and design robust containment measures.

6.2. Application for the Rock Brittleness

To further the rationality of the proposed brittleness indexes for different rock types, the datasets of uniaxial and triaxial tests on two rock types, including granite and coal specimen, are collected from the literature [26,27]. The brittleness for the two rock types

is calculated using the proposed formula. Herein, the brittleness index B7 is selected to verify the accuracy of the proposed brittleness index, as shown in Figure 11, both B7 and Bnew have the same variation trend with the confining pressure, characterizing by gradual decline. Evidently, the Bnew conforms to the law of exponential decline, which better reflects the brittleness characteristics of the two rocks. Therefore, the proposed brittleness index can be used to evaluate the other rock types.

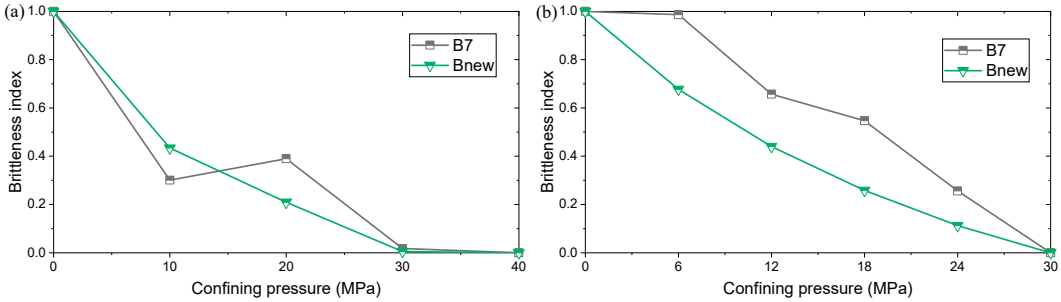

Figure 11. Application of the proposed brittleness index for different rock types: (**a**) Granite; (**b**) Coal specimen.

A brittleness index is proposed in this study, which describes the characteristics of stress-strain curves at different stages by considering the pre-peak plastic deformation and post-peak failure energy of rock mass. This leads to the development of a new brittleness evaluation method that offers the following advantages: (a) Consideration of pre-peak plastic deformation: Traditional brittleness evaluation indices often overlook the pre-peak plastic deformation of rock mass. However, this method introduces a pre-peak brittleness index factor that fully takes into account the plastic deformation characteristics of rocks during the loading process. This aids in a more accurate assessment of rock brittleness. (b) Consideration of post-peak failure energy: The method also introduces a post-peak brittleness index factor, considering the total energy consumed by the rock mass during the post-peak failure process. This reflects the failure characteristics of rocks in the post-peak stage, providing more comprehensive information for evaluating rock brittleness. (c) Clear physical significance: The method is based on the analysis of stress-strain curve characteristics and provides a more physically meaningful approach to quantify rock brittleness through energy considerations. Compared to traditional empirical indices or simple parameters, this energy-based evaluation method better reflects the mechanical properties and engineering behavior of rocks.

However, the method also has limitations and drawbacks, including requirement for experimental data support. The application of this method requires experimental testing to obtain relevant parameters such as stress-strain curves and failure energy of rocks. This may entail significant experimental workload and costs, and could be subject to limitations imposed by experimental conditions.

Rock brittleness evaluation methods are essential tools in rock engineering, offering valuable information for a wide range of engineering applications [28]. This section aims to provide an overview of the engineering applications of these methods, emphasizing their importance in optimizing engineering designs, assessing stability, and predicting rock failure. The discussion also addresses the challenges associated with implementing these methods in practical engineering scenarios.

(a) Optimization of Engineering Designs

Rock brittleness evaluation methods are instrumental in the optimization of engineering designs, particularly in areas such as tunneling, mining, and geotechnical engineering. By assessing the brittleness characteristics of rocks, engineers can make informed decisions about support systems, excavation methods, and blasting techniques. This leads to more

efficient and cost-effective designs that minimize the risk of rock failures and ensure the long-term stability of structures.

(b) Stability Analysis of Rock Structures

The evaluation of rock brittleness is crucial for the stability analysis of rock structures, including slopes, foundations, and underground excavations. By considering the brittleness indexes, engineers can assess the potential for brittle failure and identify areas prone to rock fracturing. This information helps in designing appropriate reinforcement measures and slope stabilization techniques, minimizing the risk of catastrophic failures and ensuring the safety of infrastructure [29].

(c) Prediction of Rock Failure

Rock brittleness evaluation methods aid in predicting rock failure, providing early warnings and allowing for proactive measures to mitigate potential hazards. By quantifying the brittleness characteristics of rocks, engineers can assess their susceptibility to failure under different loading conditions. This information is vital for designing monitoring systems, implementing preventive measures, and developing reliable risk management strategies [30].

(d) Challenges and Future Directions

The practical implementation of rock brittleness evaluation methods faces several challenges, including the accurate quantification of brittleness indexes, the heterogeneity of rock formations, and the need for advanced testing equipment. Future research should focus on developing standardized testing protocols, integrating multiple evaluation methods, and improving the applicability of these methods to diverse geological conditions. Additionally, advancements in non-destructive testing techniques and numerical modeling can enhance the accuracy and efficiency of rock brittleness assessments.

7. Conclusions

(1) The advantages and disadvantages of different approaches based on mineral composition, strain, stress, elastic parameter, and energy to determine the rock brittleness are summarized. Most brittleness indexes also fail to reflect some characteristics about the complete stress-strain curves. Therefore, it is necessary to propose a brittleness index that can simultaneously reflect the pre-peak and post-peak curve characteristics and capture the elastic and plastic deformation features during the rock failure process.

(2) Considering the plastic deformation in pre-peak and failure energy in post-peak, an energy-based brittleness index is proposed in this study. The triaxial test data of red-bed sandstone and cyan sandstone under different conditions is used to evaluate the rock brittleness. For red-bed sandstone, both in the natural state and under saturated conditions, the brittleness index of red-bed sandstone decreases with increasing confining pressure. However, the brittleness of red-bed sandstone under saturated conditions is lower compared to its natural state. For cyan sandstone, the brittleness of cyan sandstone decreases with increasing confining pressure, and freezing-thawing action can reduce the brittleness of the rock.

(3) To validate the rationality of the proposed brittleness index, three brittleness indexes, including stress-based, strain-based, and energy-based brittleness indexes, are selected to compare with the proposed brittleness index. For red-bed sandstone, the proposed brittleness index under natural conditions exhibits the maximum values at all confining pressures, with the lowest value observed for B7. The four brittleness indexes consistently characterize the brittleness of the red-bed sandstone under natural conditions. Under saturated conditions, the brittleness indexes exhibit different patterns of variation. For cyan sandstone, the three brittleness indexes—B7, B9, and Bnew—under natural conditions exhibit a similar trend in characterizing the brittleness of the cyan sandstone, while the trend of B17 is essentially opposite to the previous three indexes. Under freezing-thawing conditions, the variation patterns of

the three brittleness indexes, B7, B9, and Bnew, are similar. Similarly, the trend of B17 is essentially opposite to that of the previous three indexes.

Author Contributions: Conceptualization, X.Y., T.W. and Y.G.; methodology, X.Y., T.W. and Y.G.; validation, T.W. and Y.G.; data curation, T.W.; writing—original draft preparation, X.Y., T.W. and Y.G.; writing—review and editing, X.Y., T.W. and W.J.; supervision, M.H.; project administration, Y.W.; funding acquisition, T.W. and M.H. All authors have read and agreed to the published version of the manuscript.

Funding: The work was funded by the National Natural Science Foundation of China (No. 42002268); Science and technology program of Tibet Autonomous Region (XZ202202YD0007C, XZ202301YD0034C); Open Fund of Badong National Observation and Research Station of Geohazards (No. BNORSG-202204).

Institutional Review Board Statement: Not applicable.

Informed Consent Statement: Not applicable.

Data Availability Statement: The data that support the findings of this study are available on request from the corresponding author. The data are not publicly available due to privacy.

Conflicts of Interest: Author Xiaopeng Yue was employed by the company Zhongguan Chenhua Petroleum Engineering Co., Ltd. The remaining authors declare that the research was conducted in the absence of any commercial or financial relationships that could be construed as a potential conflict of interest.

References

1. Rybacki, E.; Meier, T.; Dresen, G. What controls the mechanical properties of shale rocks?—Part II: Brittleness. *J. Pet. Sci. Eng.* **2016**, *144*, 39–58. [CrossRef]
2. Meng, F.Z.; Wong, L.N.Y.; Zhou, H. Rock brittleness indices and their applications to different fields of rock engineering: A review. *J. Rock Mech. Geotech. Eng.* **2021**, *13*, 221–247. [CrossRef]
3. Rahimzadeh Kivi, I.; Zare-Reisabadi, M.; Saemi, M.; Zamani, Z. An intelligent approach to brittleness index estimation in gas shale reservoirs: A case study from a western Iranian basin. *J. Nat. Gas Sci. Eng.* **2017**, *44*, 177–190. [CrossRef]
4. Bailey, A.H.E.; Jarrett, A.J.M.; Wang, L.; Reno, B.L.; Tenthorey, E.; Carson, C.; Henson, P. Shale brittleness within the Paleoproterozoic Isa Superbasin succession in the South Nicholson region, Northern Australia. *Aust. J. Earth Sci.* **2022**, 1–18. [CrossRef]
5. Wen, T.; Tang, H.; Wang, Y. Brittleness evaluation based on the energy evolution throughout the failure process of rocks. *J. Pet. Sci. Eng.* **2020**, *194*, 107361. [CrossRef]
6. Wen, T.; Tang, H.M.; Wang, Y.K.; Ma, J.W. Evaluation of methods for determining rock brittleness under compression. *J. Nat. Gas Sci. Eng.* **2020**, *78*, 103321.
7. Zhang, Y.; Feng, X.-T.; Yang, C.; Han, Q.; Wang, Z.; Kong, R. Evaluation Method of Rock Brittleness under True Triaxial Stress States Based on Pre-peak Deformation Characteristic and Post-peak Energy Evolution. *Rock Mech. Rock Eng.* **2021**, *54*, 1277–1291. [CrossRef]
8. Wen, T.; Wang, Y.; Tang, H.; Zhang, J.; Hu, M. Damage Evolution and Failure Mechanism of Red-Bed Rock under Drying–Wetting Cycles. *Water* **2023**, *15*, 2684. [CrossRef]
9. Altindag, R. The evaluation of rock brittleness concept on rotary blast hold drills. *J. S. Afr. Inst. Min. Metall.* **2002**, *102*, 61–66.
10. Altindag, R. Assessment of some brittleness indexes in rock-drilling efficiency. *Rock Mech. Rock Eng.* **2010**, *43*, 361–370. [CrossRef]
11. Gao, M.; Li, T.; Meng, L. An Evaluation Method of Rock Brittleness Based on the Prepeak Crack Initiation and Postpeak Stress Drop Characteristics. *Math. Probl. Eng.* **2021**, *2021*, 5639649. [CrossRef]
12. Kuang, Z.; Qiu, S.; Li, S.; Du, S.; Huang, Y.; Chen, X. A New Rock Brittleness Index Based on the Characteristics of Complete Stress–Strain Behaviors. *Rock Mech. Rock Eng.* **2021**, *54*, 1109–1128. [CrossRef]
13. Shi, X.; Wang, M.; Wang, Z.; Wang, Y.; Lu, S.; Tian, W. A brittleness index evaluation method for weak-brittle rock by acoustic emission technique. *J. Nat. Gas Sci. Eng.* **2021**, *95*, 104160. [CrossRef]
14. Jarvie, D.M.; Hill, R.J.; Ruble, T.E.; Pollastro, R.M. Unconventional shale-gas systems: The Mississippian Barnett Shale of north-central Texas as one model for thermogenic shale-gas assessment. *AAPG Bull.* **2007**, *91*, 475–499. [CrossRef]
15. Khan, N.M.; Ahmad, M.; Cao, K.; Ali, I.; Liu, W.; Rehman, H.; Hussain, S.; Rehman, F.U.; Ahmed, T. Developing a New Bursting Liability Index Based on Energy Evolution for Coal under Different Loading Rates. *Sustainability* **2022**, *14*, 1572. [CrossRef]
16. Zhao, Z.; Liu, Z.; Lu, C.; He, T.; Chen, M. Brittleness evaluation based on shale fracture morphology. *J. Nat. Gas Sci. Eng.* **2022**, *104*, 104679. [CrossRef]
17. Wan, C.; Song, Y.; Li, Z.; Jiang, Z.; Zhou, C.; Chen, Z.; Chang, J.; Hong, L. Variation in the brittle-ductile transition of Longmaxi shale in the Sichuan Basin, China: The significance for shale gas exploration. *J. Pet. Sci. Eng.* **2021**, *209*, 109858. [CrossRef]

18. Zheng, Z.; Zheng, H.; Zhao, J.; Liu, Z.; Feng, G.; Qiu, S. Ductile–brittle quantitative evaluation of rock based on post-peak properties under true triaxial stress. *Géoméch. Geophys. Geo-Energy Geo-Resour.* **2023**, *9*, 81. [CrossRef]
19. Li, Y.; Zhou, L.; Li, D.; Zhang, S.; Tian, F.; Xie, Z.; Liu, B. Shale Brittleness Index Based on the Energy Evolution Theory and Evaluation with Logging Data: A Case Study of the Guandong Block. *ACS Omega* **2020**, *5*, 13164–13175. [CrossRef]
20. Gong, F.Q.; Wang, Y.L. A New Rock Brittleness Index Based on the Peak Elastic Strain Energy Consumption Ratio. *Rock Mech. Rock Eng.* **2022**, *55*, 1571–1582. [CrossRef]
21. Wang, W.; Wang, Y.; Chai, B.; Du, J.; Xing, L.; Xia, Z. An Energy-Based Method to Determine Rock Brittleness by Considering Rock Damage. *Rock Mech. Rock Eng.* **2022**, *55*, 1585–1597. [CrossRef]
22. Zhang, X.; Xu, J.; Shaikh, F.; Sun, L.; Cao, Y. Rock Brittleness Evaluation Index Based on Ultimate Elastic Strain Energy. *Processes* **2022**, *10*, 1367. [CrossRef]
23. Munoz, H.; Taheri, A.; Chanda, E.K. Fracture Energy-Based Brittleness Index Development and Brittleness Quantification by Pre-peak Strength Parameters in Rock Uniaxial Compression. *Rock Mech. Rock Eng.* **2016**, *49*, 4587–4606. [CrossRef]
24. Kaunda, R.B.; Asbury, B. Prediction of rock brittleness using nondestructive methods for hard rock tunneling. *J. Rock Mech. Geotech. Eng.* **2016**, *8*, 533–540. [CrossRef]
25. Wen, T.; Tang, H.; Huang, L.; Wang, Y.; Ma, J. Energy evolution: A new perspective on the failure mechanism of purplish-red mudstones from the Three Gorges Reservoir area, China. *Eng. Geol.* **2020**, *264*, 105350. [CrossRef]
26. Zhang, J.; Ai, C.; Li, Y.W.; Che, M.G.; Gao, R.; Zeng, J. Energy-Based Brittleness Index and Acoustic Emission Characteristics of Anisotropic Coal under Triaxial Stress Condition. *Rock Mech. Rock Eng.* **2018**, *51*, 3343–3360. [CrossRef]
27. Zhang, J.; Ai, C.; Li, Y.W.; Zeng, J.; Qiu, D.Z. Brittleness evaluation index based on energy variation in the whole process of rock failure. *Chin. J. Rock Mech. Eng.* **2017**, *36*, 1326–1340.
28. Tarasov, B.; Potvin, Y. Universal criteria for rock brittleness estimation under triaxial compression. *Int. J. Rock Mech. Min. Sci.* **2013**, *59*, 57–69. [CrossRef]
29. Wang, S.; Chen, Y.; Ni, J.; Liu, G.; Fernández-Steeger, T.M.; Xu, C. Mechanical Characteristics and Mechanism of Granite Subjected to Coupling Effect of Acidic Corrosion and Freeze-Thaw Cycles. *J. Earth Sci.* **2021**, *32*, 1202–1211. [CrossRef]
30. Wang, Y.; Li, C.; Cai, Z.; Zhu, G.; Zhou, J.; Yao, W. Mechanical Behaviors of Anchorage Interfaces in Layered Rocks with Fractures under Axial Loads. *J. Earth Sci.* **2023**, *34*, 354–368. [CrossRef]